Discover Geoscience

Research

Novel method to determine bedrock from a single sensor based seismic reflection signal using Haar wavelet transform

N. E. Ramesh[1] · **S. Pushpa Mala**[2]

Received: 14 November 2023 / Accepted: 27 August 2024
Published online: 17 September 2024

Abstract
The determination of bedrock depth is crucial across various earth sciences and related fields. Geophysical techniques, notably the continuous wavelet transform, are increasingly employed to map subsurface bedrock structures. This method allows the transformation of 1D time domain seismic reflection signals into a 2D image, providing time–frequency representations for feature extraction. Leveraging the advantages of wavelet theory, particularly the Haar wavelet known for its simplicity and compact support, this study utilizes continuous Haar wavelet local maxima lines to enhance bedrock analysis. Seismic reflection data is acquired using an extremely sensitive geophone as a receiver along with a high dynamic range data logger. The Common Midpoint (CMP) approach, coupled with optimized offset distances, is utilized to ensure robust data quality and signal strength. Simple sources, such as a sledgehammer, generate sound waves for data collection prior to borehole drilling, correlating acquired data with lithogeological information. This research emphasizes the significance of adjusting parameters like sampling frequency, choice of wavelet, and optimal offset distances. The methodology employed, involving a single geophone, a one-channel data recorder, and a basic sledgehammer as a sound source, offers an inexpensive, straightforward, and non-invasive approach. The study demonstrates the effectiveness of Haar wavelet local maxima lines in accurately determining bedrock depth, producing results closely aligned with both predicted and actual depths.

Keywords Bedrock · Wavelet · Haar · Seismic · Local maxima lines

1 Introduction

In geophysical exploration, traditional methods such as resistivity and magnetic surveys often face limitations when it comes to achieving high-resolution mapping of geological boundaries at greater depths. These techniques may lack the necessary resolution to delineate subsurface structures effectively [1]. For shallow sediments and near-surface investigations, seismic refraction and reflection techniques are preferred as they offer superior resolution and detail in identifying geological and structural interfaces [2]. Seismic reflection is recognized for its ability to provide high-resolution images of subsurface features, making it a valuable method for exploring and understanding geological formations [3]. However, the conventional approach to seismic reflection involves multiple channels and sensors, which increases both the cost and complexity of data acquisition and processing compared to other geophysical methods [4]. To address these challenges, this study proposes an innovative method that utilizes a single sensor and datalogger channel for seismic data collection. This approach aims to simplify the process and reduce costs while maintaining the ability to obtain

✉ N. E. Ramesh, ner@mcehassan.ac.in; S. Pushpa Mala, pushpa.mala-ece@dsu.edu.in | [1]Department of E&I Engineering, Malnad College of Engineering, Hassan 573202, India. [2]Department of ECE, Dayananda Sagar University, Bengaluru 562112, India.

high-resolution images of the subsurface. By employing wavelet transforms, this method can convert a one-dimensional (1D) seismic signal into a two-dimensional (2D) image, facilitating the identification of bedrock and other geological features with greater efficiency and precision [5–7].

Wavelet transforms have become a powerful tool in geophysics for improving the analysis and interpretation of complex data sets. The Haar wavelet offers distinct advantages in the analysis of seismic reflection data, making it a valuable tool for determining subsurface structures such as bedrock. Wavelet transforms, including both the discrete wavelet transform (DWT) and the continuous wavelet transform (CWT), enable the decomposition of complex signals into components that can be more easily analyzed and interpreted [8–12]. The DWT is well-suited for tasks such as noise reduction and data compression, which are crucial when dealing with large volumes of seismic data. In contrast, the CWT provides enhanced capabilities for capturing detailed local fluctuations within a signal, allowing for more refined feature extraction [13–18]. In the context of bedrock determination, the application of wavelet transforms allows for the transformation of 1D seismic data into a 2D representation, which improves the visualization and identification of bedrock interfaces and geological boundaries [19–21]. The Haar wavelet, with its straightforward and efficient approach, proves particularly effective in extracting key features from seismic data, thereby enhancing the accuracy of subsurface imaging. Additionally, integrating wavelet techniques with other geophysical methods can significantly enhance the quality of seismic data interpretation, leading to more accurate and cost-effective mapping of bedrock and other geological features [22, 23]. This study's innovative use of a single sensor combined with wavelet transform techniques represents a promising advancement in geophysical exploration, offering a more accessible and economical solution for detailed subsurface investigations.

1.1 Literature survey

Understanding bedrock depth is crucial for numerous applications in geotechnical and civil engineering [24]. Various methods are employed to determine this depth, each offering different advantages and limitations regarding accuracy, cost, speed, and invasiveness. A review of the literature reveals several prevalent techniques used in geotechnical surveys to ascertain bedrock depth [25]

1. Seismic refraction and reflection: this method involves sending seismic waves into the ground and analyzing their velocity and amplitude as they reflect off subsurface layers. It is relatively fast, non-invasive, and provides a general estimate of bedrock depth. However, its effectiveness can be influenced by the complexity of subsurface conditions and the presence of noise [26].
2. Electrical resistivity imaging (ERI): ERI measures variations in the electrical conductivity of subsurface materials. It can differentiate between soil and bedrock based on their contrasting conductivities. ERI is non-invasive and cost-effective but may require dense data sampling for accurate results.
3. Ground penetrating radar (GPR): GPR utilizes radar pulses to image subsurface structures and can identify material property variations. While it is non-invasive and provides fast results, its penetration depth and resolution may be limited by the presence of high-conductivity materials and soil conditions.
4. Magnetic methods: these methods measure variations in the Earth's magnetic field caused by differences in subsurface materials. They are non-invasive and relatively low-cost but may not directly reveal bedrock depth due to the broad nature of magnetic field changes.
5. Cone penetration testing (CPT): CPT involves pushing a cone-shaped probe into the ground and measuring resistance changes. It can provide detailed data on soil layering and resistance, potentially indicating bedrock presence. While fast and cost-effective, CPT may not directly measure bedrock depth and can be invasive.
6. Microgravity surveys: these surveys measure variations in gravitational forces due to different subsurface densities, which can suggest bedrock depth. They are non-invasive but require specialized equipment and expertise, making them less accessible for routine surveys.

Each technique has its strengths and weaknesses, and often a combination of methods or a comprehensive geophysical survey is employed to achieve a more accurate understanding of bedrock depth. The choice of technique depends on geological conditions, project requirements, available budget, and technology. Recent advancements in data processing and technology have significantly enhanced the precision and effectiveness of these methods, leading to more accurate and cost-effective solutions for geotechnical surveys [26–30].

Among the various techniques, wavelet transforms have emerged as a significant advancement in geophysical data analysis. Wavelet transforms decompose complex signals into components that are easier to analyze, allowing for detailed examination of local fluctuations within seismic data. This capability is particularly beneficial for identifying subtle changes in subsurface structures and improving the accuracy of bedrock depth determination. The application of wavelet transforms, such as the Haar wavelet, provides enhanced resolution and feature extraction from seismic reflection data, contributing to more precise subsurface imaging [31]. By transforming 1D seismic signals into 2D images, wavelet transforms facilitate better visualization and identification of geological boundaries and bedrock interfaces [32]. Integrating wavelet techniques with traditional geophysical methods can offer a comprehensive approach to geotechnical surveys, balancing accuracy, cost, and efficiency in bedrock mapping and subsurface investigations [33, 34].

1.2 Present seismic reflection methodology

To detect bedrock and its depth to the surface, or any other subsurface layers of the earth, the current technology requires many sensors. Recorded each sensor's signals were layered, and Fig. 1 illustrates how the signals' amplitudes changed over time. These abrupt changes in amplitude are thought to mark the subsurface border. Calculating the signal's velocity is necessary to ascertain the depth of the bedrock or layers. This process necessitates people, machinery, and highly competent software programmers, as well as being time consuming and costly. The paper provides a cost-effective, simple, and efficient method that eliminates the need to determine velocity of the subsurface layers [35].

1.3 Proposed methodology

Seismological concepts are applied in the exploration geophysics technique known as reflection seismology to infer characteristics of the Earth's subsurface from reflected seismic waves]. A controlled seismic energy source is necessary for the technique. The most adaptable method for subsurface imaging was seismic reflection, which is based on wavelet transform that utilizes two-dimensional local maxima lines. Sound waves are created and transferred into the subsurface, where they are refracted or reflected by rocks with different physical properties and density of the sub surface layers. Sledgehammer weighing 3 kg is employed in this project as a source. A datalogger with a single channel and a sensor (a geophone) are used. A single channel's raw data (signal) is used for identifying bedrock. The raw data is processed using the MATLAB wavelet toolbox's Haar wavelet to decompose it from a 1D signal into two-dimensional information. Local maximum lines are created when frequency atoms (small non-stationary reflected waves where each dot of the two-dimensional information) from the seismic reflection signal bounce off the bedrock. These lines aid in determining the depth of the bedrock. Bedrock depth can be determined using Haar wavelet local maxima lines without the use of complex mathematics.

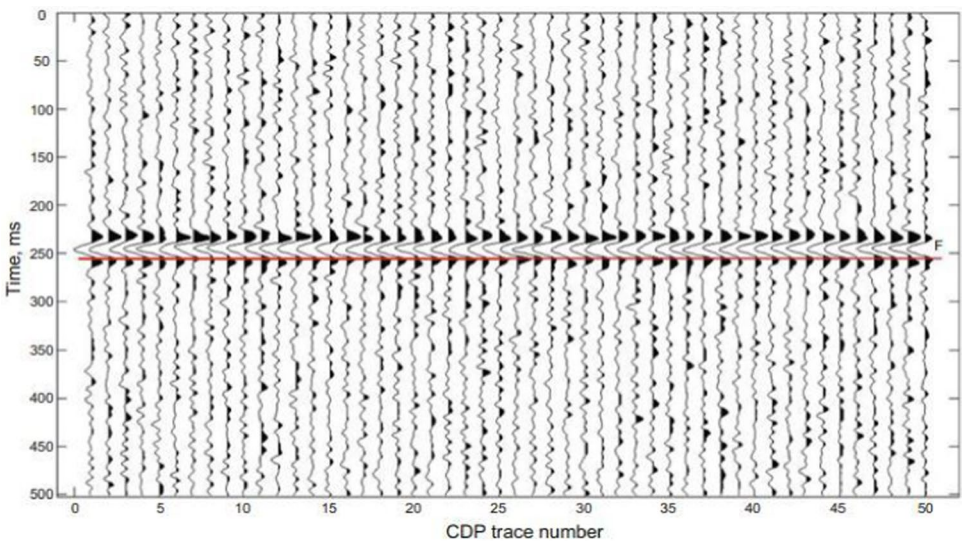

Fig. 1 Stacked recorded signals

1.4 Haar wavelet transform

The simplest wavelet is the Haar wavelet. Haar wavelets are related to the Haar transform in discrete form, which is a mathematical procedure. The Haar transform is the model for all other wavelet transforms [36].

A. Haar Scaling Function.

The scaling function equation is:

$$\Psi(x) = \Psi(2x) + \Psi(2x - 1)$$

The only function that satisfies this is:

$$\Psi(x) = 1 \text{ if } 0 \leq x \leq 1$$

$\Psi(x) = 0$ otherwise as shown in Fig. 2

B. Translation and Dilation of $\Psi(x)$

$$\Psi(2x) = 1 \text{ if } 0 \leq x \leq 1/2$$

$$\Psi(2x) = 0 \text{ elsewhere}$$

$$\Psi(2x - 1) = 1 \text{ if } 1/2 \leq x \leq 1$$

$$\Psi(2x - 1) = 0 \text{ elsewhere}$$

so, the sum of the two functions is then:

Wavelets are constructed by taking differences of scaling functions as shown in Fig. 3.

$$\Psi(x) = X\, k\, (-1)\, k\, c1 - k\, \Psi(2x - k).$$

$$\Psi(\mathbf{x}) = \sum_K C_1 - K^{\Phi}(2x - k)$$

Differencing is caused by the (− 1) k, the (-1)k term causes differencing by alternating the sign of the coefficients, leading to alternating positive and negative contributions from neighboring data points. so, the basic Haar wavelet is as follows as shown in Fig. 4

As in Fig. 5. seismology is comprised of a source, earth's subsurface layered seismic reflection or refraction signal, highly sensitive sensor (geophone), datalogger, and software to interpret the collected data.

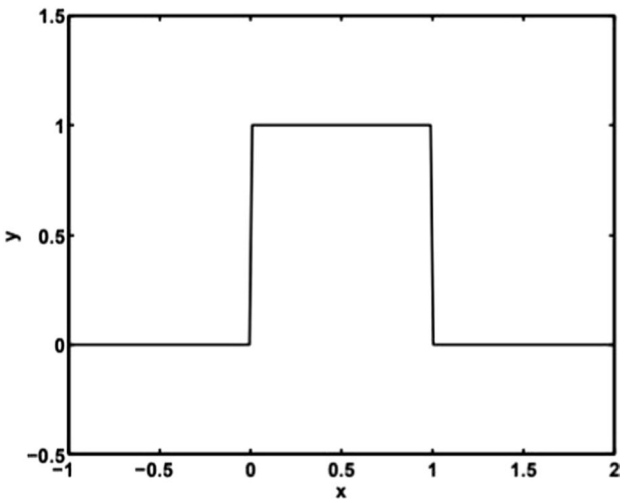

Fig. 2 Haar wavelet scaling function

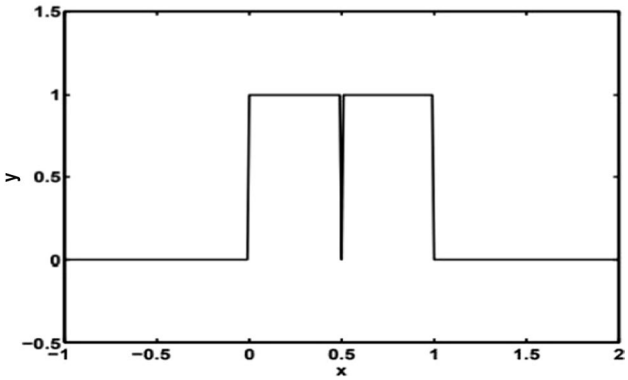

Fig. 3 Haar wavelet with translation and dilation

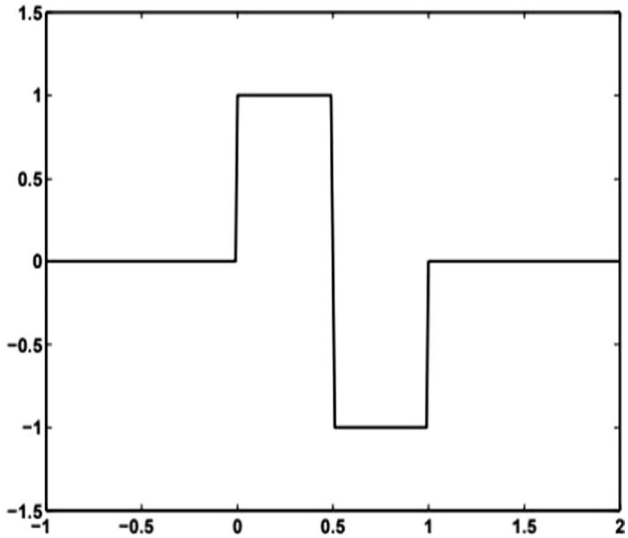

Fig. 4 Basic Haar wavelet

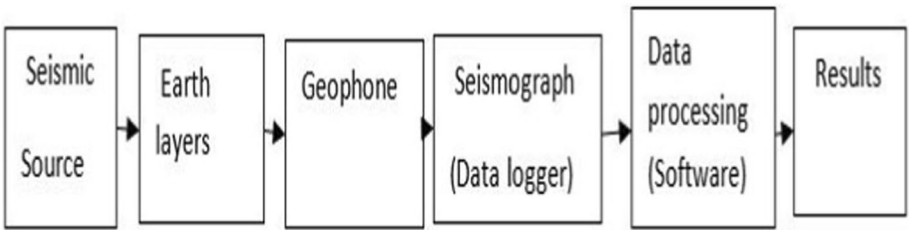

Fig. 5 Block diagram of seismology

1.5 VI. Seismic Reflection

The seismic reflection method measures how long it takes for a seismic wave to move from its source to the ground, bounce back to the surface, and be picked up by a receiver. This duration of time is called Two-way travel(TWT)time. The most challenging aspect of seismic reflection surveys is the transformation of travel time to depth (TWTT to depth) [37–39].

The interval velocity is determined different depth intervals to yield an average velocity v^{I}.

$$VI = \frac{\sum_{i=1}^{n} Zi}{\sum_{i=1}^{n} \tau i} = \frac{\sum_{i=1}^{n} Vi.\tau i.}{\sum_{i=1}^{n} \tau i} \; or \; VI = \frac{Z_n}{T_n} \tag{1}$$

Zn = Total thickness of the top n layers.
Tn = total one-way travel time through the n layers.

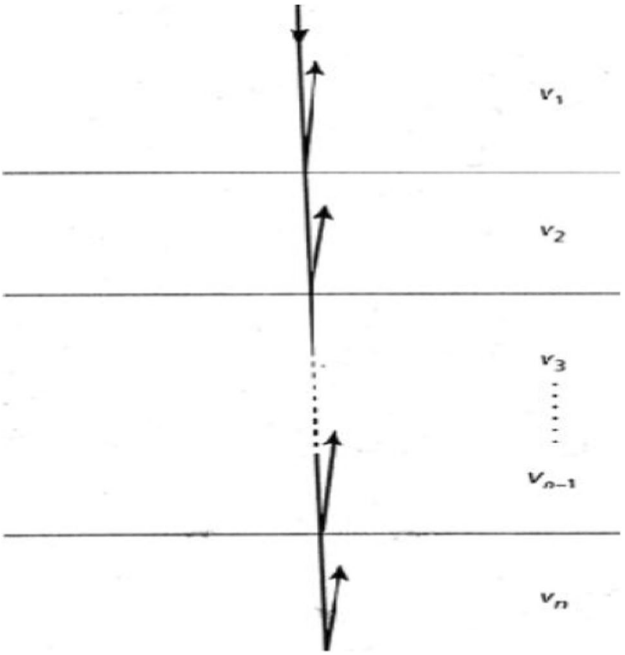

Fig. 6 Vertical reflected ray paths in a horizontally layered subsurface

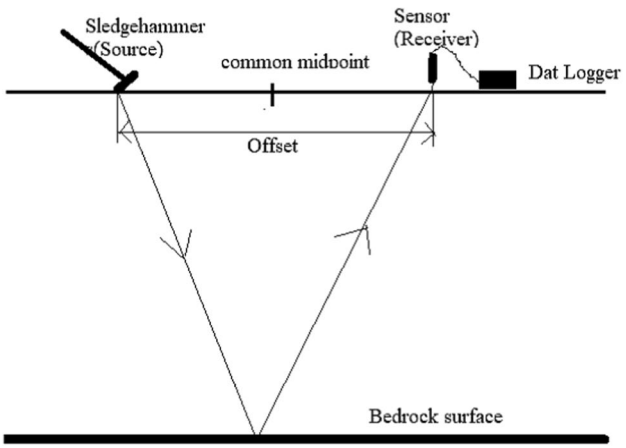

Fig. 7 The source—receiver layout and corresponding ray paths for a common mid-point

Total all velocity is determined by Eq. 1

The equation for the travel time T of the reflected ray as shown in Fig. 6 from a shot point to a detector at a horizontal offset x is given by:

$$T = \frac{(X^2 + Z^2)^{1/2}}{V} \tag{2}$$

T is determined at offset distance x using Eq. 2.

1.6 Common mid-point for single layer

The two-way seismic reflection line as well as the offset distance are both illustrated in Fig. 7. In the case of reflection seismic data, it is commonly considered that the distance between the shot (source) and the receiver (geophone) is the same at the halfway point. During the process of collecting CMP records, the source and receiver are moved in opposite directions so that the midpoint between them remains unchanged. As a result, the distance between the source and receiver expands. We will obtain multiple signals at the same location if we keep hitting the same spot with the hammer

repeatedly. If the surface of the location is not completely flat and dry, the data quality may suffer. During the process of collecting data, there should be no ambient noise, either from urban or rural settings. After many trial and error attempts, it was found that the three-meter offset distance was the best option. This is because it was the most practical choice for this work, as if the offset distance is less than three meters, it shows less than the actual depth of the bed rock, and if it is more than three meters, the bed rock depth appears to increase due to the longer two-way travelling time. This strategy is also referred to as the Common-Depth-Point method (CDP). CMP is preferred, even though both names are equally valid and accurately describe the method in question. Because the use of CMP setup and wavelet local maxima lines to calculate the depth of bed rock complicated equations is no longer required.

1.7 MTSS – 1001 geophone (sensor)

MTSS-1001 is a compact geophone. This geophone is a one-component variant. It has a high sensitivity, a large dynamic range, and the capacity to function in any gravitational orientation [40]. According to the MTSS-1001 specs, the frequency range is 1-300 Hz, hence a sampling frequency greater than twice is required based on the Nyquist Criterion, so 1 kHz was chosen. For ground installations, the MTSS-1001 comes with a screw tail nail as shown in Fig. 8. This geophone is extremely sensitive at low frequency applications compare to conventional geophones. Electric current through the MET is primarily dictated by hydrodynamic electrolyte motion caused by mechanical disturbances from the outside. On MET electrodes, the rate of a chemical reaction far outpaces the rate of reactant delivery. In this context, a reactant concentration gradient occurs during reactions in the MET, and charge transfer occurs inside an immobile electrolyte due to molecular diffusion from one electrode to another. Molecular diffusion is accompanied by convective ion transfer when a liquid flow under the influence of inertia forces [30]. As a result, the rate at which reactants are delivered to electrodes is increased. The current running through the MET is varying because of the external change in motion.

2 results and discussions

2.1 Field setup and data logging

Correct field configuration, such as sensor coupling to earth and choosing a flat, dry surface, is crucial to obtaining the best possible data quality, as Fig. 9 illustrates. We make use of an iron peg that has a diameter of one inch and a length of ten inches to enable the sensor is to be clamped into place on the surface. This helps to stabilize the sensor so that it does not shake while it is collecting data. The data logger, the sensor, and the Toughbook that is used to visualize the data are all located on the receiver side. A common midpoint is marked at the center of the source and the receiver. A three-kilogram sledgehammer is being used as the source on the side opposite to the receiver. Data logger manufactured by Symmetric Research Company called PARCH4 is employed. In this work, only one channel and one geophone are employed to record raw data from the field. Data is logged and processed using various sample frequencies and offset

Fig. 8 MTSS-1001 geophone

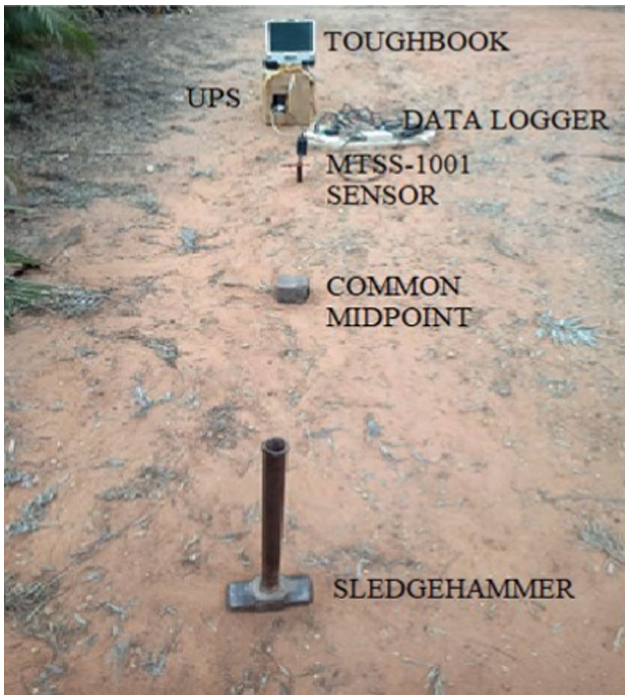

Fig. 9 Data acquisition field setup

distances to correlate lithological data. It has been shown that the proper data acquisition settings are 1,000 Hz sampling frequency and a three-meter offset distance. The signal will begin to be transmitted as soon as we strike the surface with the sledgehammer. We generate a greater number of signals for both ease of use and the ability to select the signal with the highest possible quality. These signals (data) are saved in a Toughbook (Field use Laptop). The software known as MATLAB wavelet toolbox is utilized to conduct supplementary analyses on them later.

3 Results

The main goal of our study is to identify the top surface of the bedrock. To achieve this objective, the owners of borehole rigging machines were consulted to determine where they intended to drill boreholes to formers for the purpose of ground water exploration in agriculture. Prior to digging the boreholes at each of the ten locations, data is recorded. When drilling boreholes, note the depth at which bedrock was seen or the point at which the overburden soil above the bedrock ended. In order to prevent the borehole from collapsing, metal pipe must be introduced into the overburdened soil, that is, the depth from the bed rock to the surface [23]. Metal pipe, sometimes referred to as casing, must be installed to keep boreholes from collapsing. To our investigation, these measurements of the depth of the bedrock will serve as a reference. After processing the data with Haar wavelet 1D continuous wavelet local maxima lines, we compared these lithological data with the predicted bedrock depth.

The MATLAB wavelet toolbox software is used to conduct an analysis on all these raw data. The wavelet toolbox that we are looking at contains a variety of wavelets transforms, such as Morlet, Mexican hat, and Haar, amongst others. A series of analyses using a variety of wavelets are used and all wavelet transforms are not suitable for all the work, selection of wavelet transform for application is most important. As a result, chosen Harr 1D continuous wavelet from MATLAB toolbox. This 1D signal(data) is converted into a 2D information by the wavelet transform. This allows us to see the lines that correspond to the local maxima. As shown in the Figs. 10,11,12,13, 14, and 15, a group of frequency atoms is responsible for the formation of these local maxima lines. The local maxima lines are created by frequency atoms, each frequency atoms are corresponding to different reflected signal with different frequencies. These frequency atoms are produced by multiple reflected signals from the boundaries of the various layers. The raw data have analyzed with different sampling frequency, different offset, and other wavelets available in MATLAB wavelet toolbox, it is confirmed that Haar wavelet is the t wavelet transform for our work out of all the wavelet transforms. The sampling frequency of 1000 Hz (as per Nyquist Criterion) with three-meter offset are optimum parameters. The X-axis samples and local maxima lines in the Haar wavelet are nearly identical to the bedrock measured in feet. The depth of the bed rock can be calculated

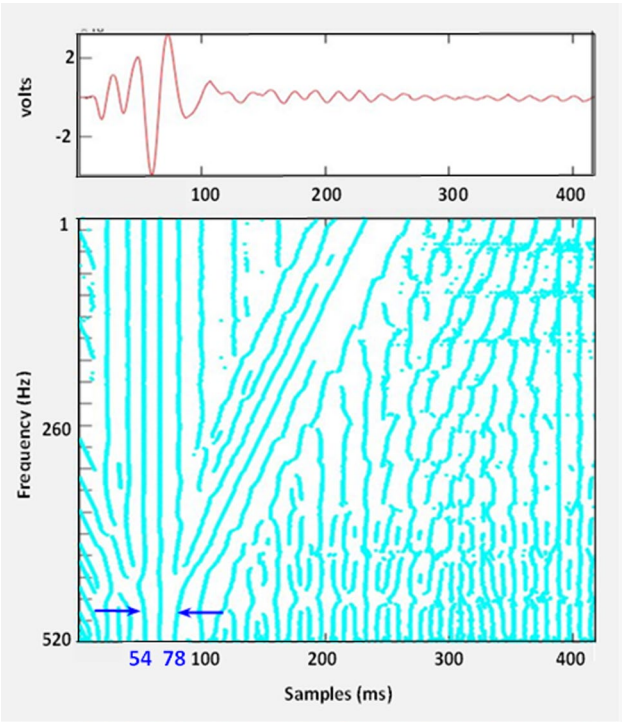

Fig. 10 Raw data and analyzed data of borehole one

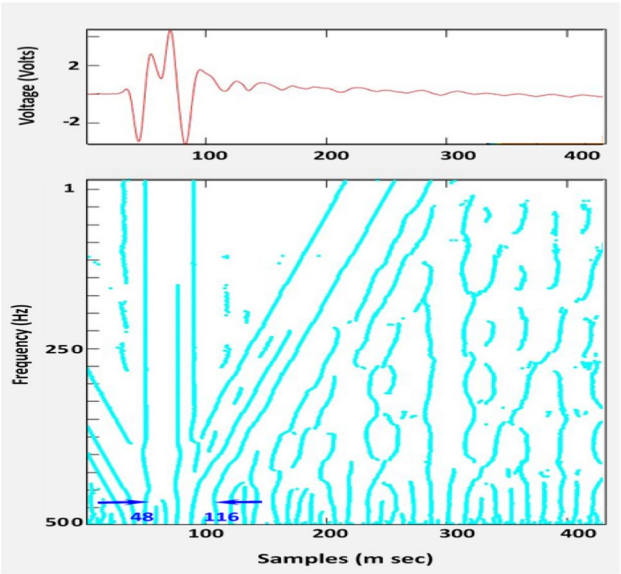

Fig. 11 Raw data and analyzed data of borehole two

using the signals (data) that have already been logged. The top surface is revealed by the first vertical line that from the local maxima line. Additionally, an end inclined local maxima line without a discontinuity reveals the topography of the bedrock. The sample numbers in the x-axis where it is necessary to note the initial line and last line positions. As seen in the Figs. 11,12,13,14,15 and 16 arrow marks are used to denote these line positions. The depth of the bedrock is determined by subtracting the first line sample number from the end line sample numbers. Actual bedrock depth based on lithological (After boreholes have been drilled) data and predicted bedrock depth from the local maxima lines are remarkably close to one each other. Seven of the ten results from boreholes processed data are displayed. The outcomes from the other three boreholes are identical to those we obtained at a bedrock depth of almost forty feet.

Depth of the bedrock of different boreholes are determined by local maxima lines of the Harr wavelet. The novel method of determining the bedrock as follows. From 1D raw data, Fig. 10 shows a processed image of the Local maximum lines. The first continuous vertical line formed by surface waves denotes the surface at sample point 54

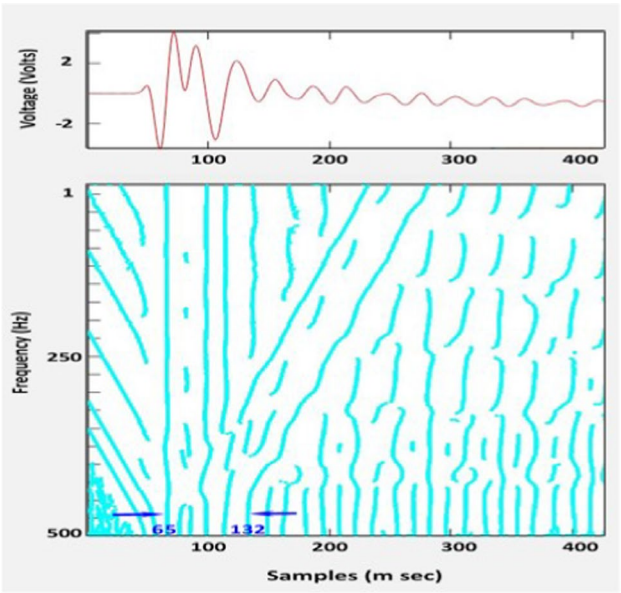

Fig. 12 Raw data and analyzed data of borehol

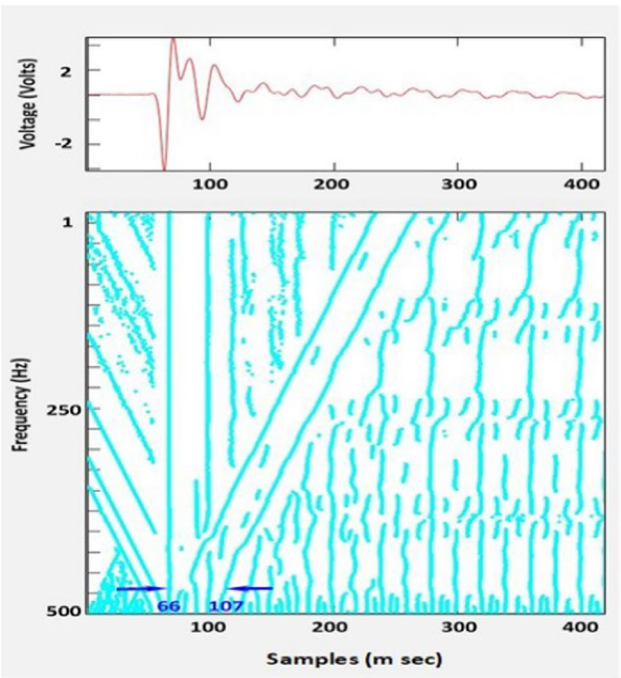

Fig. 13 Raw data and analyzed data of borehole four

and the last vertical line formed by reflected from boundaries the bed rock indicates at sample point 78, where the arrow lines are marked so that 78–54 = 24 feet. Regarding the lithological data, the real depth is 25 feet, whereas the depth determined from the local maxima lines is 24 feet. When the same process is applied on boreholes 2, 3, 4, 5 and 6, we obtained the results that are presented in the Table 1.

Errors in determining the bedrock's depth shown in Fig. 16 and in relation to borehole number 7, where data was obtained when the surface was excessively moist. It is difficult to predict the depth due to the inadequate quality of the data. The lithological data indicates that the bed rock is 42 feet deep; however, due to the low quality of the data, it is not possible to estimate the bed rock because there are no continuous vertical local maxima lines. This directly means that having high-quality data is essential to avoiding analysis errors.

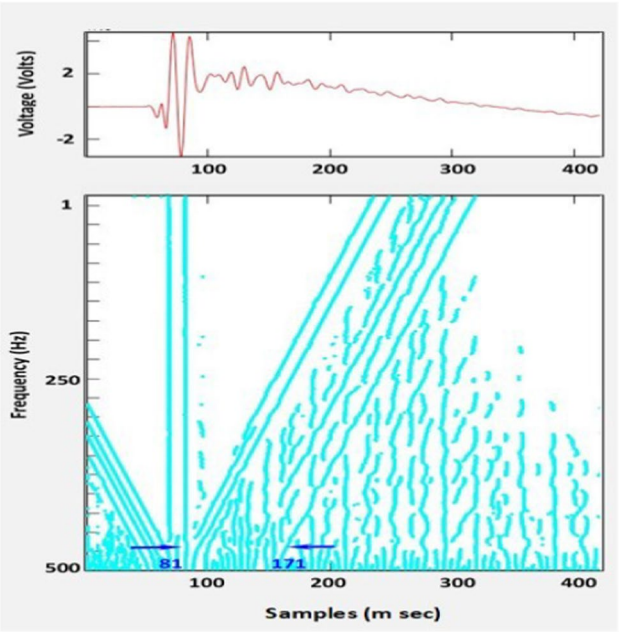

Fig. 14 Raw data and analyzed data of borehole five

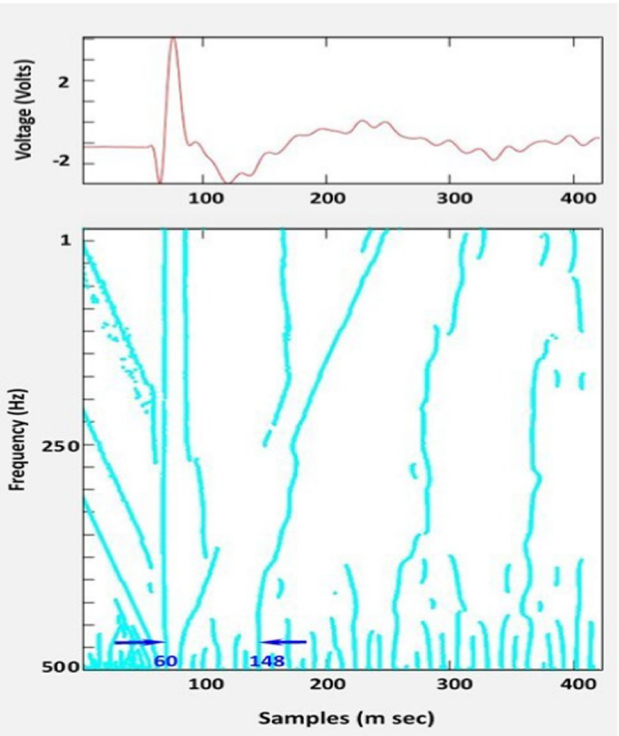

Fig. 15 Raw data and analyzed data of borehole six

4 Conclusion

This study aimed to determine the bedrock depth in the Hassan district of Karnataka, India, leveraging the varied topologies of ten selected locations. The research highlighted the efficiency and effectiveness of this method in bedrock localization, crucial for preventing structural damage in various constructions like multistory buildings, roads, and metro railway pillars. Utilizing a single channel datalogger and geophone proved cost-effective and less labor-intensive compared to invasive techniques, making it a viable option for engineering projects. The versatility of

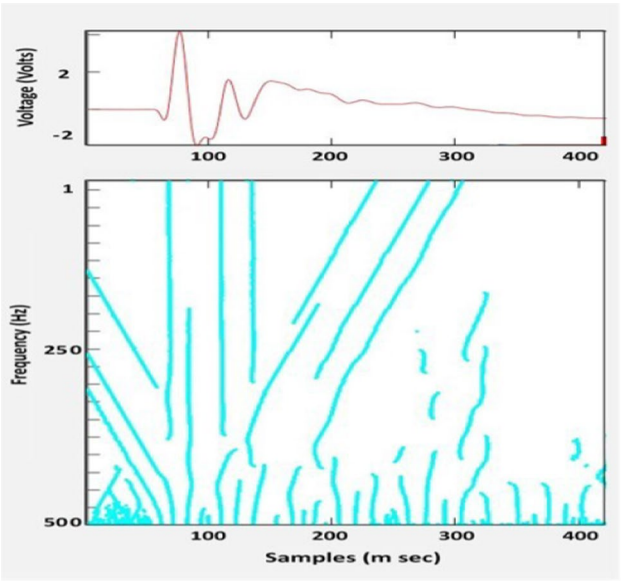

Fig. 16 Raw data and analyzed data of borehole seven

Table 1 Depth calculations

Borehole No	Figure No	Sample number of first line	Sample number of second line	Depth calculated in feet	Actual depth in feet
1	10	54	78	24	25
2	11	48	116	68	65
3	12	65	132	67	66
4	13	66	107	41	40
5	14	81	171	90	88
6	15	60	148	88	86

employing different methods based on site geology, target size, and engineering concerns underscores the importance of a comprehensive understanding before initiating geophysical investigations. This method correlated with drill data in our investigation, despite the possibility of slight differences between expected and actual bedrock depths, especially in flat, dry terrain. Given the circumstances, establishing offset parameters, adjusting sampling frequency, and utilizing the Haar wavelet proved to be the best options, establishing a benchmark for subsequent bedrock localization techniques.

Author contributions Ramesh N. E. contributed to the design and modeling, performed the simulations, and verified the results. Pushpa Mala S. proposed the design, individually verified the results, and equally contributed to the design, modeling, and simulation. All authors contributed equally to the work.

Funding The authors received no financial support for the research, authorship, and/or publication of this article.

Data availability Not applicable.

Declarations

Consent for publication I confirm that informed consents, including Consent to Participate and Consent to Publish, were obtained from all participants involved in this study. Each participant was provided with clear and comprehensive information about the study's objectives, procedures, and benefits. Additionally, participants were informed about the possibility of publication."Data sets generated during the current study are available from the corresponding author on reasonable request.

Competing interests The authors declared no potential competing of interest with respect to the research, authorship, and/or publication of this article.

References

1. Nath RR, Kumar G, Sharma ML, Gupta SC. Estimation of bedrock depth for a part of Garhwal Himalayas using two different geophysical techniques. Geo Sci lett. 2018;5:9. https://doi.org/10.1186/s40562-018-0108-9.
2. Grinsted A, Moore JC, Jevrejeva S. Application of the cross wavelet transform and wavelet coherence to geophysical time series. Nonlinear Proc Geophys. 2004;11:561–6.
3. Wapenaar K, Ghose R, Toxopeus G, Fokkema J. The wavelet transforms as a tool for geophysical data integration. Integr Comput-Aided Eng. 2005;12:5–23.
4. L. Alperovich, L. Eppelbaum, V. Zheludev, J. Dumoulin, F. Soldovieri, M. Proto, M. Bavusi,, and A. Loperte. 2012. A new combined wavelet methodology applied to GPR and ERT data in the Montagnole experiment (French Alps). Geophysical Research Abstracts. 14: EGU2012–6338
5. Ruixue Sun, Ayse Kaslilar, Christopher Juhlin, "High resolution seismic reflection PP and PS imaging of the bedrock surface below glacial deposits in Marsta, Sweden" Journal of Applied Geophysics 198 (2022) 104572. https://www.elsevier.com/locate/jappgeo.
6. Fkirin MA, Badawy S, El Deery MF. Seismic Refraction Method to Study Subsoil Structure. Jf Geol Geophys. 2016;5:5. https://doi.org/10.4172/2381-8719.1000259.
7. Salas-Romero S, Malehmir A. Ian snowball and bojan brodic", geotechnical site characterization using multichannel analysis of surface waves: a case study of an area prone to quick-clay landslides in southwest sweden", near surface geophysics published by john wiley & sons ltd on behalf of european association of geoscientists and engineers. Near Surface Geophy. 2021;19:699–715.
8. Poggi V, Giardini d. Time–frequency–wavenumber analysis of surface waves using the continuous wavelet transform" springer, pure appl. Geophysics. 2013;170:319–35. https://doi.org/10.1007/s00024-012-0505-5.
9. Schmelzbach C, Horstmeyer H, Juhlin C. Shallow 3D seismic-reflection imaging of fracture zones in crystalline rock. Geophysics. 2007;72:6.
10. Opara C, Adizua OF, Ebeniro JO. Near-surface seismic velocity model building from first arrival travel-times - a case study from an onshore, Niger delta field. Univers J Physics Applicat. 2018;12(1):1–10.
11. Onyebueke EO, Manzi MSD, Durrheim RJ. High-resolution shallow reflection seismic integrated with other geophysical methods for hydrogeological prospecting in the Nylsvley nature reserve South Africa. J Geophysics Eng. 2018;15:2658–73.
12. Ahmad MN, Rowell P, Sriburee S. Detection of fluvial sand systems using seismic attributes and continuous wavelet transform spectral decomposition: case study from the Gulf of Thailand. Marine Geophysical Res. 2013. https://doi.org/10.1007/s11001-014-9213-0.
13. Miguel TG, López-Benítez TZ, Enggee Lim MA, Limin Yu. A review of wavelet analysis and its applications: challenges and opportunities. IEEE Access. 2022. https://doi.org/10.1109/ACCESS.2022.3179517.
14. Kumar P, Georgiou EF. Wavelet analysis for geophysical applications. Rev Geophys. 1997;35:385–412.
15. Ker S, GonidecGibert YD, Marsset B. Multiscale seismic attributes: a wavelet-based method and its application to high-resolution seismic and ground truth data. Geophys J Int. 2011;187:1038–54. https://doi.org/10.1111/j.1365-246X.2011.05207.x.
16. Kris Innanen, "Seismic processing with continuous wavelet transform maxima" CREWESResearch Report — Volume 25 (2013).
17. Ibrahim A, Md Noor MJ, Ibrahim MN, Ahmad J, Ahmad A. Maximum shear modulus evaluation based on continuous wavelet transform of bender element test. J Physics. 2019. https://doi.org/10.1088/1742-6596/1349/1/012019.
18. Haleem DA, Kesserwani G, Caviedes-Voullième D. Haar wavelet-based adaptive finite volume shallow water solver. J Hydroinform. 2015;17(6):857–73.
19. Khorshid SZ, Owiad JI. Sub-surface investigation of khashim al-ahmer gas field using seismic reflection data Iraqi. J Sci. 2015;56(1C):774–84.
20. Palmer D. A new direction for shallow refraction seismology: integrating amplitudes and travel times with the refraction convolution section. Geophys Prospect. 2001;49:657–73.
21. Palmer D. Measurement of rock fabric in shallow refraction seismology. Explor Geophys. 2001;32:307–14. https://doi.org/10.1071/EG01307.
22. Lambang Wahyu Nugrohoa) and Dewi Retno Sari Saputro, "Signal Analysis with Continuous Wavelet Transform" Proceedings of the 6th National Conference on Mathematics and Mathematics Education AIP Conf.Proc.2577,020043–1–020043–5; https://doi.org/10.1063/5.0096025.
23. Adiela UP, Emudianughe, JAkomolafe MT. Low velocity layer mapping using seismic refraction technique in 'a' field, etche, rivers state Nigeria. Int J Innov Res. 2016;2:10.
24. Peggy Subirats, Jean Dumoulin, Vincent Legeay and Dominique Barba, "Automation Of Pavement Surface Crack Detection Using The Continuous Wavelet Transform". 1424404819/06/ ©2006 IEEE.
25. Hutapea FL, Tsuji T, Katou M, Asakawa E. Data processing and interpretation schemes for a deep-towed high-frequency seismic system for gas and hydrate exploration. J Nat Gas Sci Eng. 2020. https://doi.org/10.1016/j.jngse.2020.103573.
26. Cichostępski K, Kwietniak A. Relative amplitude preservation in high-resolution shallow refraction seismic: a case study from Fore-Sudetic Monocline. Poland Acta Geophysica. 2019;67:77–94.
27. Ivanov J, Miller RD, Lacombe P, Johnson CD, Lane JW. Delineating a shallow fault zone and dipping bedrock strata using multichannel analysis of surface waves with a land streamer. Soc Explorat Geophys. 2006;71(5):A39–42.

28. Li W, Yue D, Shenghe Wu, Shu Q, Wang W, Long T, Zhang B. Thickness prediction for high-resolution stratigraphic interpretation byfusing seismic attributes of target and neighboring zones with an SVR algorithm. Marine Petrol Geolog. 2019. https://doi.org/10.1016/j.marpetgeo.2019.104153.
29. Ren Z, Kalscheuer T. Uncertainty and resolution analysis of 2D and 3D inversion models computed from geophysical electromagnetic data. Surveys Geophysics. 2020. https://doi.org/10.1007/s10712-019-09567-3.
30. Yan F, Shangguan W, Zhang J, Bifeng H. Depth-to-bedrock map of China at a spatial resolution of 100meters. Sci Data. 2020. https://doi.org/10.1038/s41597-019-0345-6.
31. Yang G, Li QJ, Zhan YJ, Wang KCP, Wang C. Wavelet based macrotexture analysis for pavement friction prediction. J Civil Eng. 2018;22(1):117–24. https://doi.org/10.1007/s12205-017-1165-x.
32. Alfonso Fernández-Lavín & Efraín Ovando-Shelley, "S-wave velocity assessment using time-scale approaches with wavelets." Proceedings of the 20th International Conference on Soil Mechanics and Geotechnical Engineering– Rahman and Jaksa (Eds). 2022 Australian Geomechanics Society, Sydney, Australia,
33. Prokoph A, Agterberg FP. Wavelet analysis of well-logging data from oil source rock, Egret Member, offshore eastern Canada. Am Associat Petrol Geolog. 2000;84(10):1617–32.
34. Ucan ON, Serhat Seker A, Albora M, Ozmen A. Separation of magnetic fields in geophysical studies using a 2-D multi-resolution Wavelet analysis approach. J Balkan Geophys Soc. 2000;3(3):53–8.
35. Zhao L, Han D-H, Yao Q, Zhou R, Yan F. Seismic reflection dispersion due to wave-induced fluid flow in heterogeneous reservoir rocks. Soc Explorat Geophys. 2015;80(3):D221–35.
36. Schimmack M, Nguyen S, Mercorelli P. Anatomy of haar wavelet filter and its implementation for signal processing. Science Direct. 2016;49(6):099–104.
37. Tsuru T, Park JO, No T, Kido Y, Nakahigashi K. Visualization of attenuation structure and faults in incoming oceanic crust of the Nankai Trough using seismic attenuation profiling. Earth Planets Space. 2018. https://doi.org/10.1186/s40623-018-0803-y.
38. Li Q, Guochen Wu. 2D multi-parameter waveform inversion of land refraction seismic data obtained from the particle-motion response from the vertical geophone. Acta Geophys. 2020;68:377–88. https://doi.org/10.1007/s11600-020-00403-6.
39. Leopold M, Dethier D, Völkel J, Raab T, CorsonRikert T, Caine N. Using geophysical methods to study the shallowsubsurface of a sensitive alpine environment, niwot ridge, colorado front range. Arctic Antarctic Alpine Res. 2018;40(3):519–30.
40. Zaitseva DL, Avdyukhinaa SY, Agafonova VM, Academician AS, Bugaev E, Egorova V. A molecular-electronic hydrophone for low-frequency research of ambient noise in the world ocean. Doklady Earth Sci. 2018;483(2):1579–81.